NASA Technical Memorandum 85781

A ROBUST PSEUDO-INVERSE SPECTRAL FILTER APPLIED TO THE EARTH RADIATION BUDGET EXPERIMENT (ERBE) SCANNING CHANNELS

LEE M. AVIS, RICHARD N. GREEN,
JOHN T. SUTTLES, AND SHASHI K. GUPTA

MARCH 1984

National Aeronautics and
Space Administration

Langley Research Center
Hampton, Virginia 23665

A ROBUST PSEUDO-INVERSE SPECTRAL FILTER APPLIED TO THE EARTH RADIATION BUDGET EXPERIMENT (ERBE) SCANNING CHANNELS

ABSTRACT

Computer simulations of a least squares estimator operating on the ERBE scanning channels are discussed. The estimator is designed to minimize the errors produced by non-ideal spectral response to spectrally varying and uncertain radiant input. The three ERBE scanning channels cover, respectively, a shortwave band from 0.18 to 5 microns, a longwave band from 5 to 50 microns, and a "total" band from 0.15 to beyond 1000 microns, from which the pseudo-inverse spectral filter estimates the radiance components in the shortwave band and a longwave band (5 to 1000 microns).

The radiance estimator draws on instantaneous field of view (IFOV) scene-type information supplied by another algorithm of the ERBE software, and on a priori probabilistic models of the responses of the scanning channels to the IFOV scene types for given Sun-scene spacecraft geometry.

The pseudo-inverse spectral filter has been found to be stable, tolerant of errors in scene identification and in channel response modeling, and, in the absence of such errors, to yield minimum variance and essentially unbiased radiance estimates.

INTRODUCTION

The "radiation budget" is the solar irradiance absorbed in a given region of the Earth-atmosphere system minus the radiant emittance to space averaged over a specified time. Knowledge of how the radiation budget varies temporally and spatially over the globe is fundamental to understanding the energy sources and sinks within the Earth-atmosphere system.

Satellite observations of the radiation budget date from 1959, with the Explorer 7 providing the first. There followed TIROS 2, 3, 4, and 7; Nimbus 2; ESSA 3, 5, 7, and 9; Nimbus 3; ITOS 1; NOAA 1; and Nimbus 6 and 7. The Earth Radiation Budget Experiment (ERBE), benefiting from the experience gained by these earlier efforts, is expected to yield greatly improved measurement accuracy through emphasis on instrument characterization and calibration, both pre-flight and in-flight. Furthermore, the three satellites of the ERBE system should reduce errors caused by aliasing of Earth flux field variations with sampling periodicities.

The National Aeronautics and Space Administration (NASA) is planning the ERBE mission for the mid-1980's to provide an initial research data set and to demonstrate the feasibility of routine monitoring of radiation budget parameters for use in climate analyses and projections. The ERBE radiometers will be flown on two of NOAA's Sun-synchronous TIROS N satellites and a NASA-developed mid-inclined Earth Radiation Budget Satellite (ERBS) to be launched from the Space Shuttle.

The three satellites are to have nearly identical ERBE instrumentation:

(1) A total wave band solar monitor

(2) Limb-to-limb Earth viewing radiometers, one for the shortwave band (0.18 to 5 microns) and one for the total band

(3) Medium field of view (10° Earth central angle) nadir viewing radiometers with the same bands as the limb-to-limb sensors

(4) Three Earth scanning radiometers covering, respectively, a shortwave band (0.18 to 5 microns), a longwave band (5 to 50 microns), and a "total" band (0.15 to 1000+ microns).

The principal mission of the scanners is to monitor emitted and solar reflected radiant exitance from 250- to 1000-kilometer regions. Any use of these data sets to improve understanding of the energy sources and sinks and their action on the atmosphere and oceans could conceivably be misled not only by the magnitude of the errors in the data, but also, a fortiori, any correlations the errors may have with the processes under study. The scanning channels do not respond uniformly to all wavelengths within their respective wavebands; thus, to the extent that variable spectral response is not accounted for, there will be scanner measurement errors correlated with spectral changes in the scenes in view--notably, the spectral changes associated with changes in cloudiness, snow cover, vegetation, and solar zenith angle.

Some of the planned ERBE scientific investigations which could be susceptible to variable scanner spectral response are:

(1) Albedo-solar zenith angle dependence as a seasonal feedback mechanism in climate models

(2) Effect of cloudiness on radiation budget

(3) Radiation budget-atmospheric circulation correlations

(4) Radiation parameterization in global circulation models (GCM's)

(5) Radiation budget as diagnostic for GCM's.

In this paper, we present a technique aimed at (1) reducing scanner spectral response effects and (2) quantifying the remaining errors of this kind in terms of explicit models of the scanner channels' spectral response and stochastic models of the Earth spectral fields. We feel that making the models and assumptions explicit is necessary for the intelligent use of the data products, and also allows updating the technique whenever it is necessary or desirable to alter the models because of changes in the instrument characteristics or improvement in our knowledge of the Earth spectra.

BACKGROUND

Description of the ERBE Scanner

The scanning channels are configured as three parallel telescopes which scan the Earth from limb to limb. The lines of sight are confined to a plane perpendicular to the spacecraft (nominal circular orbit) velocity vector. For special, occasional studies, the scan plane is rotated about the local vertical to other orientations for brief periods. In the principal or nominal scan mode, the scan period is 4 seconds, which assures sampling overlap from scan line to scan line. Sampling overlap along the scan line is also realized by a sampling rate per channel of 30 hertz. The instantaneous fields of view for all scanning channels measure, at the spacecraft, 3° along scan and 4.5° along ground track. The fields of view (clipped diamonds) project to the Earth at nadir as nearly coincident areas of dimensions 47 by 37 km for the ERBS mid-inclination satellite, and 65 by 51 km for the TIROS satellites.

The telescopes employ cassegrain optics with polished aluminum primary and secondary mirrors. The shortwave channel has a filter and a window of Suprasil-W fused quartz, one-half millimeter and one millimeter thick, respectively. The longwave channel has a diamond filter. The total channel, although not filtered, still suffers appreciable spectral nonuniformity by double reflection off the mirrors. The current preliminary models of the spectral responses of the three channels are shown in figures 1.a-1.f. The spectral absorption of the thermistor flake detector is factored into the response curves.

Fortunately, inferrence of the longwave radiance is not solely dependent on the longwave channel; the total and shortwave channels in combination yield good longwave radiance estimates, in part because these two channels have very

similar spectra curve shapes in the near ultraviolet and the visible bands. This spectral similarity derives from the nearly ideal spectral transmittance of Suprasil-W in the near ultraviolet and visible, and from the presence of aluminum mirrors in the optical trains of both the total and shortwave channels.

The longwave channel filter was chosen to be spectrally similar to that of Nimbus 6 and 7 ERB longwave channels, so that more direct connection might be made between ERBE and ERB measurements than could be made with spectrally dissimilar channels. The longwave channel, as well as offering a measure of redundancy, is intended to assist in cloud detection and classification. The redundancy feature is significant; the shortwave channel cannot be calibrated in flight against blackbody simulators as the longwave and total channels are, and Suprasil-W transmittance in the near ultraviolet is known to degrade under ultraviolet and energetic electron flux. (Preflight flux aging is expected to desensitize the Suprasil to orbital flux.) In-flight checks of the shortwave channel are made by observations of space, an incandescent lamp, and of the Sun's reflection from the "Mirror Attenuator Mosaic" (MAM), which functions as a diffuser of solar flux. The MAM and the incandescent lamp are not considered of the same order of accuracy and precision as the blackbody simulators, however. The total channel is also checked against space and the MAM, as well as a blackbody simulator. The longwave channel is in-flight calibrated against space and, as mentioned before, a blackbody simulator.

The Scene Identification Algorithm

Evidently, the uncertainties in estimating radiance inputs to channels with nonuniform spectral response cannot be bounded, much less minimized, unless the uncertainties in the spectral content of the inputs are bounded in some sense. The ERBE scene identification algorithm, developed for the purpose of correcting for the anisotropy of the Earth's outgoing radiation, is also applicable to the scanner spectral correction problem.

The scene viewed by the scanner is classified, pixel by pixel, as water; land, but not desert; snow; desert; land-water mix; land-snow mix; water under partly cloudy sky; non-desert land under partly cloudy sky; desert under partly cloudy sky; land-water mix under partly cloudy sky; land-snow mix under partly cloudy sky; water under mostly cloudy sky; non-desert land under mostly cloudy sky; desert under mostly cloudy sky; land-water mix under mostly cloudy sky; land-snow mix under mostly cloudy sky; or overcast sky. The clear sky scene types, the first six in the above list, are considered to have cloud amounts from 0 to 5 percent, the partly cloudy scene types from 5 to 50 percent, the mostly cloudy scene types from 50 to 95 percent, and the overcast condition more than 95 percent cloud amount. The mixed undersurfaces range from 33 to 67 percent to 67 to 33 percent composites of the two pure undersurface types. In general, undersurface types are defined to resolution elements 2.5° by 2.5° in latitude and longitude. Cloud amount, however, is determined pixel by pixel.

The undersurface type distribution over the globe is defined a priori, while the cloud amount in the instantaneous field of view (IFOV) is constructed from the scanner measurements.

As discussed in a following section, statistical populations of radiation spectra, generated by radiation transfer models, are associated with the scene types (sub-divided into polar, mid-latitude, and tropical regions and according to Sun-IFOV-spacecraft angles). The pseudo-inverse spectral filter operates on numerically integrated channel responses to each spectrum and on statistical parameters of the spectral population to form optimal radiance estimates as a linear combination of the channel measurements.

In view of the dependence of the spectral correction on the constructed IFOV scene type, it seems appropriate to describe the ERBE scene identification algorithm in some detail.

The scene identification algorithm relies upon models which predict the shortwave and longwave radiances to be observed by ERBE from each scene type. The predictive models are constructed from archived Nimbus 7 ERB scanner data and THIR 11-micron window channel observations. The window channel serves to estimate cloud cover fraction by means of an objective threshold technique, while the ERB scanner measurements accumulate statistics on the radiances associated with each scene type as functions of the exiting ray direction and, for shortwave, the incident solar ray direction (ref. 1). From the predictive model thus constructed, the ERBE scene identification algorithm computes the probability that each ERBE scanner IFOV overlays a "clear," "partly cloudy," "mostly cloudy," and an "overcast" area. The undersurface is specified according to geography.

Taylor and Stowe (ref. 1) have concluded that except for land areas at night (often classed as cloudy), the cloud amounts derived from THIR are accurate to 10 to 20 percent, and that the amount of low clouds is the most difficult to estimate accurately.

As things stand at present, we must expect appreciable confusion between clear targets and those underneath warm (i.e., low contrast in the infrared) clouds. Plans are being made to use GOES visible and infrared measurements of ERB/THIR targets to improve the clear surface-warm cloud discrimination. The poor discrimination between clear land and clouds at night is not considered to seriously degrade either radiation anisotropy modeling or spectral response correction.

Although the Nimbus 7 ERB shortwave and longwave scanning channels pass the same nominal wavebands as the ERBE shortwave and longwave scanners, there are some possibly significant differences in detail which, of course, tend to soften the credibility of ERBE scene identification built on ERB data. The ERB shortwave channel optical train includes two mirrors, a 2-millimeter-thick Suprasil-W filter, and a pyroelectric detector. The ERB longwave channel has two mirrors plus a third chopper/beam diverter mirror, a diamond filter very similar to the ERBE longwave filter, and a pyroelectric detector. The spectral responses of the Nimbus 7 scanning channels have not been measured.

THEORY OF THE SPECTRAL CORRECTION

The spectral radiance $L(\lambda)$ incident on the ith scanning channel (i=1,2,3) produces a measurement given by

$$Y_i = \int_0^\infty r_i(\lambda)\, L(\lambda)\, d\lambda + \varepsilon_i \tag{1}$$

where $r_i(\lambda)$ is the spectral response, λ is the wavelength (μm), and ε_i is the measurement error arising from all sources except uncertainty in the normalized spectral radiance,

$$1(\lambda) = L(\lambda) \Big/ \int_0^\infty L(\lambda)\, d\lambda \tag{2}$$

The measurement Y_i characterizes the integral of spectral radiance $L(\lambda)$ over a waveband labeled "i," defined by:

i	waveband (μm)	channel/waveband name
1	0 - 5	shortwave
2	5 - ∞	longwave
3	0 - ∞	total

The spectral response $r_i(\lambda)$ is dimensionless and, for an ideal instrument, is unity within the channel waveband and zero elsewhere. Losses in the optical train of the actual instrument reduce the spectral response in the passband to a nonuniform value below unity (fig. 1), and shortwave filter and window transmission at 50 μm and beyond leaks longwave[1] into the shortwave measurement (fig. 2).

The shortwave channel is predominantly sensitive to reflected solar energy, and the longwave to Earth/atmosphere emitted energy.

The shortwave radiance,

$$L_1 = \int_0^{5\ \mu m} L(\lambda)\, d\lambda \tag{3}$$

and the longwave radiance,

---

[1]Cess, Robert D.: Private communication.

$$L_2 = \int_{5\ \mu m}^{\infty} L(\lambda)\, d\lambda \tag{4}$$

are estimated by

$$\hat{L}_j = \sum_{i=c}^{3} [B_{ji}\ Y_i];\quad j = 1,2;\quad c = \begin{cases} 1, & \text{day IFOV} \\ 2, & \text{night IFOV} \end{cases} \tag{5}$$

where $\hat{L}_1$ and $\hat{L}_2$ are the estimates of L_1 and L_2, and the matrix of B's is a variable to be determined for each IFOV. The estimate error is

$$\eta_j = \hat{L}_j - L_j \tag{6}$$

We choose to minimize the expected value of $\eta_1^2 + \eta_2^2$, or

$$\sum_{j=1}^{2} \eta_j^2 = \sum_{j=1}^{2} \left[\left(\sum B_{ji}\ Y_i\right) - L_j\right]^2 \tag{7}$$

a necessary condition for which is

$$\frac{\partial}{\partial B_{nm}} \left[E\left(\sum_{j=1}^{2} \eta_j^2\right)\right] = 0;\quad n = 1,2;\quad m = c,\ldots,3$$

or, since the operators E (expectation) and $\frac{\partial}{\partial B_{nm}}$ commute,

$$E\left\{\frac{\partial}{\partial B_{nm}} \sum_{j=1}^{2} \eta_j^2\right\} = 0 \tag{8}$$

or, by use of equation (7),

$$E\left\{2\left(\sum_{i=c}^{3} [B_{1c}\ Y_i] - L_1\right) Y_m \cdot \delta_n^1 + 2\left(\sum_{i=c}^{3} [B_{2i}\ Y_i] - L_2\right) Y_m \cdot \delta_n^2\right\} = 0$$

where the δ's are Kronecker deltas; thus

$$E\left\{\left(\sum_{i=c}^{3}\left[B_{ni}\ Y_i\right] - L_n\right) Y_m\right\} = 0; \quad n = 1,2; \quad m = c,\ldots,3 \tag{9}$$

which are two sets of 4-c equations in 2x(4-c) unknown B's expressing a necessary condition for minimum sum of squared error, $\eta_1^2 + \eta_2^2$. For a given IFOV, the B's are constant, thus eq. (9) becomes

$$\sum_{i=c}^{3} B_{ni}\ E\{Y_i\ Y_m\} = E\{L_n\ Y_m\} \tag{10}$$

or, in matrix notation,

$$E\{\bar{Y}\ \bar{Y}^T\}\ \bar{B}_n = E\{L_n\ \bar{Y}\} \tag{11}$$

where $n = 1$ or 2 and $\bar{Y}$ and $\bar{B}_n$ are the column vectors (dimensioned 4-c) of the Y's and B_n's. Therefore,

$$\bar{B}_n = \left[E\{\bar{Y}\ \bar{Y}^T\}\right]^{-1} E\{L_n\ \bar{Y}\} \tag{12}$$

for nonsingular $E\{\bar{Y}\ \bar{Y}^T\}$. Let

$$[B] = [\bar{B}_1\ \bar{B}_2] = \begin{cases} \begin{bmatrix} B_{11} & B_{21} \\ B_{12} & B_{22} \\ B_{13} & B_{23} \end{bmatrix} & \text{day IFOV} \\ \begin{bmatrix} B_{12} & B_{22} \\ B_{13} & B_{23} \end{bmatrix} & \text{night IFOV} \end{cases} \tag{13}$$

$$\bar{L} = \begin{bmatrix} L_1 \\ L_2 \end{bmatrix}; \qquad \hat{\bar{L}} = \begin{bmatrix} \hat{L}_1 \\ \hat{L}_2 \end{bmatrix} \tag{14}$$

Then

$$[B] = \left[E\{\bar{Y}\ \bar{Y}^T\}\right]^{-1}\ E\{\bar{Y}\ \bar{L}^T\} \tag{15}$$

and, from equation (5),

$$\hat{\bar{L}}^T = \bar{Y}^T[B] \tag{16}$$

for nonsingular $E\{\bar{Y}\ \bar{Y}^T\}$.

Equation (16) is the formal machinery for optimal radiance estimation in the presence of all instrument errors.

The integrated response A_i of the ith channel to the normalized spectral radiance $1(\lambda)$ (eq. (2)) is

$$A_i = \int_0^\infty r_i(\lambda)\ 1(\lambda)\ d\lambda; \quad i = c,\ldots,3 \tag{17}$$

and so,

$$Y_i = A_i(L_1 + L_2) + \varepsilon_i \tag{18}$$

The elements of the matrix $E\{\bar{Y}\ \bar{L}^T\}$ become

$$\begin{aligned} E\{Y_m\ L_n\} &= E\{[A_m(L_1 + L_2) + \varepsilon_m]\ L_n\} \\ &= E\{A_m\ L\ L_n\} + E\{\varepsilon_m\ L_n\}; \quad m = c,\ldots,3; \quad n = 1,2 \end{aligned} \tag{19}$$

where $L = L_1 + L_2$, the total radiance. The elements of the matrix $E\{\bar{Y}\ \bar{Y}^T\}$ become

$$E\{Y_s\ Y_m\} = E\{(A_s\ L + \varepsilon_s)(A_m\ L + \varepsilon_m)\}$$

$$= E\{A_s\ A_m\ L^2\} + E\{\varepsilon_m\ A_s\ L\} + E\{\varepsilon_s\ A_m\ L\} + E\{\varepsilon_s\ \varepsilon_m\}$$

$$s,m = c,\ldots,3 \qquad (20)$$

We note that modeled instrument noise gets into the influence matrix [B] through the last term in equation (20).

In outline, our approach to radiance estimation is to prepare the influence matrices [B] (eq. (15)) in advance of the flight for use in equation (16). In this way, demand on computer resources during operational data processing is minimized, and assurance of algorithm stability for all conditions is obtained in advance.

In general, a number of theoretically constructed Earth spectral radiances and probabilistic weights are associated with each of the scene types (subdivided into polar, mid-latitude, and tropical regions, and according to Sun-IFOV-spacecraft angles) in the repertoire of the ERBE scene identification algorithm. These fields and weights, with the scanning channels' spectral responses $r_i(\lambda)$, determine the influence matrix [B] by equations (19), (20), and (15).

Numerical instability of the algorithm is possible (but easily avoided) as a result of amplification of truncation errors by an ill-conditioned $E\{\bar{Y}\ \bar{Y}^T\}$ matrix in equation (15). The ill-condition occurs as the matrix $E\{\bar{Y}\ \bar{Y}^T\}$ approaches singularity. The following demonstrates that singularity occurs if and only if the measurement from any active channel is modeled as deterministically related to the other active channels' measurements.

Let

p = the number of model spectra in the IFOV

P_k = the model probability of the kth spectrum; $k = 1,\ldots,p$

Y_{sk} = sth channel model measurement of kth spectrum

$$\bar{X}_s = \begin{bmatrix} X_{s1} \\ X_{s2} \\ \vdots \\ X_{sp} \end{bmatrix} = \begin{bmatrix} \sqrt{P_1} & Y_{s1} \\ \sqrt{P_2} & Y_{s2} \\ & \vdots \\ \sqrt{P_p} & Y_{sp} \end{bmatrix}; \quad s = c,\ldots,3$$

Then, the elements of $E\{\bar{Y}\ \bar{Y}^T\}$ are

$$E\{Y_s\ Y_m\} = \sum_{k=1}^{p} \left[P_k\ Y_{sk}\ Y_{mk}\right] = \bar{X}_s \cdot \bar{X}_m$$

The vectors $\bar{X}_k$ are linearly dependent if and only if (ref. 2) the Gram's determinant

$$\left|\bar{X}_s \cdot \bar{X}_m\right| = 0$$

which, for three active channels, is equivalent to

$$X_{3k} = \alpha X_{2k} + \beta X_{1k};\quad \alpha,\beta \text{ constant};\quad k = 1,\ldots,p$$

or

$$Y_{3k} = \alpha Y_{2k} + \beta Y_{1k} \tag{21}$$

and for two active channels (nighttime IFOV),

$$Y_{2k} = \alpha Y_{3k} \tag{22}$$

An ideal instrument, with flat spectral response and $\varepsilon_i = 0$, would always have a singular Gram's determinant. In general, a vanishing Gram's determinant implies channel redundancy. The ERBE scanner is not sufficiently close to the ideal for channel near redundancy to pose a serious problem, but measures are taken to guard against it, nevertheless.

SPECTRAL RADIANCE MODELS

Both the longwave and shortwave spectral radiance modeling use the 106 radiosonde-measured atmosphere models taken from Wark et al. (ref. 3). The atmospheric models are profiles of pressure, temperature, water vapor, and ozone for all seasons and region types of the Northern Hemisphere, representing a very wide range of meteorological conditions.

Longwave Spectral Radiance Models

The spectral band 5 to 200 μm (2000 to 50 cm^{-1}) is divided into intervals 10 cm^{-1} wide. Atmospheric transmittance for each interval was calculated using the quasi-random band model of absorption (ref. 4). It was shown by

Tiwari and Gupta (ref. 5) that spectral transmittances of several infrared bands of atmospheric gases computed using this band model compared extremely well with laboratory measured values. Spectral parameters of individual absorption lines for the computation were obtained from the AFCRL line parameters compilation (ref. 6). Continuum absorption by water vapor and its temperature dependence have been taken into account as outlined by Roberts et al. (ref. 7). For spectral regions where bands of different constituents overlap, overall transmittances were obtained by multiplying the individual values. Absorption due to all major and minor constituents has been taken into account. Spectral radiance for overcast atmospheres is obtained by treating the cloud top as the underlying surface and considering only that part of the atmosphere which lies above the cloud. For partly cloudy conditions, the spectral radiance is obtained as the cloud-fraction weighted sum of the overcast and clear spectral radiances.

The model atmosphere is divided into homogeneous layers with boundaries at 900, 800, 700, 600, 520, 450, 400, 350, 300, 250, 150, 100, 50, 20, and 10 millibars, truncated as appropriate by the underlying surface/cloud height.

The exiting spectral radiance is output at wavelengths 5 μm, from 6 through 50 μm at 2-μm intervals, from 50 through 100 μm at 10-μm intervals, and from 100 through 200 μm at 20-μm intervals.

The spectral radiance is output at zenith angles 0°, 30°, 45°, 60°, and 75°. Spectral radiant exitance is also computed.

Shortwave Spectral Radiance Models

The upwelling spectral radiant exitance and spectral radiance at 50-km altitude, the assumed "top of the atmosphere," is computed by a method based on the finite difference method of Barkstrom (ref. 8) but generalized to include azimuthal variations, spectral variations for the entire solar spectrum, and specular reflection at the surface (ref. 9). The atmosphere is approximated locally as a plane-parallel layer with detailed vertical profiles of the physical and optical properties of the important atmospheric gases and aerosols. The cloudy atmosphere case is approximated by a plane-parallel, homogeneous layer.

The formulation of the problem is patterned after the "planetary atmosphere problem" given by Chandrasekhar (ref. 10). The system is assumed to be (1) composed of a series of plane-parallel layers so that physical properties vary in the vertical direction only, (2) illuminated at the top by a collimated beam of unpolarized solar radiation, and (3) bounded by a lower surface with specified reflective properties. Two additional simplifying assumptions are made: Thermal emission can be neglected and, for a clear atmosphere with an aerosol haze layer, polarization effects can be neglected (ref. 11).

A prohibitive computer cost would be incurred in generating spectral radiances from 106 model atmospheres with several different undersurface types for several solar zenith angles at several exit ray zenith angles and a few different exit ray azimuths. Some judicious choices must be made concerning which spectral radiant exitances are to be expanded into spectral radiances, and how to represent the remaining spectral radiances in terms of the expanded ones.

We are presently implementing and testing an objective procedure for making this decision. The procedure is founded on the (thus far tested) idea that "similarity" (in some sense) of two spectral radiant exitances bespeaks similarity of their expansion into spectral radiances. Some number of radiant exitances having minimum clustering in "similarity" would then be expanded into spectral radiances, which would best span the spectral radiance variations.

Two candidate definitions of "similarity" are being tested. The first is

$$S_{ij}^{(1)} = \int_0^{5\ \mu m} F_i(\lambda) \cdot F_j(\lambda)\ d\lambda / f_k^2$$

where

$$f_k^2 = \max\left\{\int_0^{5\ \mu m} F_j^2(\lambda)\ d\lambda,\ \int_0^{5\ \mu m} F_j^2(\lambda)\ d\lambda\right\}$$

and F_i, F_j are spectral radiant exitances; and the second is

$$S_{ij}^{(2)} = \int_0^{5\ \mu m} F_i(\lambda) \cdot F_j(\lambda)\ d\lambda \Bigg/ \sqrt{\int_0^{5\ \mu m} F_i^2(\lambda)\ d\lambda \cdot \int_0^{5\ \mu m} F_j^2(\lambda)\ d\lambda}$$

The first definition of "similarity" exacts a penalty for differences in the integrated radiant exitances, while the second does not. Both similarities range from zero to one.

Once a suitable definition of "similarity" is discovered, some number of minimally clustered spectral radiant exitances for each solar zenith angle and scene type category will be expanded into spectral radiance angular distributions. The remaining spectral radiances are to be represented by the shortwave and total channel responses as approximated by a linear interpolation between nearest neighbors in the "similarity" continuum.

The notion of "minimum clustering" requires definition. The first two spectral radiant exitances to be expanded into spectral radiances are two with the least pair-wise similarity. Each additional selected candidate minimizes the sum of the squares of its similarities to all prior selected candidates.

SIMULATION RESULTS

For the initial tests of the spectral correction algorithm, the model shortwave spectral radiances are represented as the corresponding spectral radiant exitances reduced by the Lambertian factor π. Instrument errors other than spectral dependence are not considered.

Simulation of Clear Sky Mid-Latitude Ocean Radiance Estimation

The Earth radiation fields consist of six shortwave fields and nine longwave fields which are consistent with clear mid-latitude ocean scenes. Each shortwave-longwave field pair is assigned the same probability (1/54). For the shortwave fields, the model atmospheres used in the radiation transfer calculations are Wark's (ref. 3) models 4, 29, 34, 42, 44, and 45. For the longwave fields, we use models 2, 4, 29, 32, 34, 42, 44, 45, and 101. The shortwave fields assume a solar zenith angle of 45°.

Table 1.a shows the results of 25 pseudo-random samples of the clear mid-latitude scene class. The radiance estimate errors are all very small, less than the expected instrument calibration errors. Both the sample and population error statistics are summarized in Table 1.b. The influence matrix (the B matrix of equation (16)), also displayed in Table 1.b, indicates that the longwave channel is given little influence on the radiance estimates. This is understandable in view of the longwave channel's relatively large variation in response to unit longwave radiance, with a population standard deviation of 0.02247, which is 3.9 percent of the mean longwave response, an order of magnitude more than that of the other channels for either shortwave or longwave fields.

The nighttime case is simulated by nulling the shortwave fields. The estimation errors (Tables 2.a and 2.b) are typically smaller than the daylight errors. Again the longwave channel has small influence.

Simulation of Ambiguous Clear/Hazy Mid-Latitude Ocean Radiance Estimation

The Earth radiation fields consist of the ones used for the clear sky case plus three shortwave fields consistent with haze over mid-latitude ocean and two longwave fields consistent with mid-latitude ocean covered by clouds at or lower than the 800-mbar level. For the additional longwave fields, the model atmospheres used in the radiation transfer calculations are Wark's (ref. 3) models 83 and 97, with cloud decks imposed at the 800- and 850-mbar levels, respectively. For the additional shortwave fields, we use models 2, 32, and 101. The shortwave fields assume a solar zenith angle of 45°. Each shortwave-longwave field pair is assigned the same probability.

The daytime case is summarized n Tables 3.a and 3.b. Again the estimation errors are smaller than the expected instrument calibration errors. The elements of the influence matrix are moderately different from those of the previous daylight case.

The nighttime case (Tables 4.a and 4.b) longwave estimation errors are comparable to the daylight longwave errors and to the nighttime clear ocean longwave errors. The influence matrix is nearly identical to the nighttime clear ocean matrix.

CONCLUDING REMARKS

Simulations of the spectral correction algorithm have shown it to be stable and to yield negligible errors when the scene spectral fields are well characterized. The limitations of the method derive from uncertainties in the spectral response of the channels and any lack of realism in the model spectral fields and their associated probabilities. The spectral response is of particular concern because the instruments must be characterized spectrally before flight; the in-flight calibration is not sufficient to accomplish this.

The simulation studies presented are highly idealized, but they serve to confirm the soundness of the algorithm.

REFERENCES

1. Taylor, V. Ray; and Stowe, Larry L.: Reflectance Characteristics of Uniform Earth and Cloud Surfaces Derived From NIMBUS-7 ERB. To be published in Journal of Geophysical Research, June 1984.

2. Korn, Granino A.; and Korn, Theresa M.: Mathematical Handbook for Scientists and Engineers. McGraw-Hill Book Co., 1968, p. 438.

3. Wark, D. Q.; Yamamoto, G.; and Lienesch, J. H.: Infrared Flux and Surface Temperature Determinations From Tiros Radiometer Measurements. NOAA Meteorological Satellite Laboratory, Report No. 10, 1962.

4. Wyatt, P. J.; Stull, V. R.; and Plass, G. N.: Quasi-Random Model of Band Absorption. Journal of the Optical Society of America, vol. 52, 1962, pp. 1209-1217

5. Tiwari, S. N.; and Gupta, S. K.: Accurate Spectral Modeling for Infrared Radiation. Journal of Heat Transfer, vol. 100, 1978, pp. 240-246.

6. McClatchey, R. A.; Benedict, W. S.; Clough, S. A.; Burch, D. E.; Calfee, R. F.; Fox, K.; Rothman, L. S.; and Garing, J. S.: AFCRL Atmospheric Absorption Line Parameters Compilation. AFCRL-TR-73-0096, 1973.

7. Roberts, R. E.; Selby, J. E. A.; and Biberman, L. M.: Infrared Continuum Absorption by Atmospheric Water Vapor in the 8-12 μm Window. Applied Optics, vol. 15, 1976, pp. 2085-2090.

8. Barkstrom, B. R.: A Finite Difference Method of Solving Anisotropic Scattering Problems. Journal of Quantitative Spectroscopy and Radiative Transfer, vol. 16, Sept. 1976, pp. 725-739.

9. Suttles, J. T.: Anisotropy of Solar Radiation Leaving the Earth-Atmosphere System. Ph.D. Thesis, Old Dominion University, May 1981.

10. Chandrasekhar, S.: Radiative Transfer. Oxford University Press, London, 1950.

11. Kattarwar, G. W.; Plass, G. N.; and Hitzfelder, S. J.: Multiple Scattered Radiation Emerging From Rayleigh and Continental Haze Layers. I: Radiance, Polarization, and Neutral Points. Applied Optics, vol. 15, no. 3, March 1976, pp. 632-647.

Table 1.a

]PR#0
ASSUMED FRACTIONAL TRUNCATION ERROR IN YY ELEMENTS= 1E-08

THE FIELD PROBABILITY MATRIX FILE NAME IS "OCM.Z45.PROB24"

THE SCANNER RESPONSE MATRIX FILE NAME IS "MID-LAT.OCEAN.36FIELDS"

THERE ARE 25 MEASUREMENT TRIPLETS.

ACTUAL SW	EST SW	SW ERROR	ACTUAL LW	EST LW	LW ERROR
29.633	29.686	-.052	77.040	77.068	-.028
29.777	29.815	-.037	60.437	60.467	-.030
29.641	29.688	-.046	80.417	80.457	-.039
29.633	29.686	-.052	77.040	77.068	-.028
29.777	29.816	-.038	77.040	77.070	-.030
29.330	29.358	-.027	60.532	60.556	-.023
29.777	29.812	-.034	80.417	80.459	-.041
29.562	29.509	.053	85.020	85.049	-.029
29.777	29.815	-.037	60.532	60.562	-.029
29.562	29.510	.051	97.985	98.051	-.065
29.633	29.684	-.051	60.437	60.465	-.027
29.641	29.692	-.050	60.532	60.560	-.027
29.562	29.504	.057	60.437	60.468	-.030
29.777	29.809	-.031	54.147	54.191	-.043
29.633	29.689	-.055	85.020	85.046	-.026
29.330	29.358	-.028	71.543	71.564	-.021
29.777	29.809	-.031	54.147	54.191	-.043
29.330	29.364	-.033	97.985	98.044	-.058
29.641	29.695	-.053	87.532	87.571	-.039
29.777	29.821	-.043	97.985	98.050	-.064
29.330	29.360	-.030	87.532	87.567	-.035
29.330	29.358	-.027	60.532	60.556	-.023
29.562	29.505	.056	77.040	77.071	-.031
29.777	29.819	-.042	85.020	85.049	-.028
29.633	29.687	-.054	87.532	87.571	-.039

Table 1.b

THE SW RADIANCES ARE BIASED BY .025 OR .086%

(PERCENTAGES ARE OF MEAN SW OR LW RADIANCES.)

THE LW RADIANCES ARE BIASED BY .035 OR .047 %

THE SW STANDARD DEVIATION IS .044 OR .150 %

THE LW STANDARD DEVIATION IS .037 OR .049 %

THE SW STANDARD DEVIATION EXCLUDING BIAS IS .036

THE LW STANDARD DEVIATION EXCLUDING BIAS IS .012

MATRIX OF CHANNEL INFLUENCES ON ESTIMATES

	TOTAL CHANNEL	SW CHANNEL	LW CHANNEL
SW EST	1.05237961E-03	1.6670959	-1.2049973E-03
LW EST	1.19022346	-1.35070884	-.127950311

SW POPULATION BIAS= .01389 OR .046 %

LW POPULATION BIAS= .03614 OR .048 %

SW POPULATION STD DEV= .04428 OR .149 %

LW POPULATION STD DEV= .03800 OR .050 %

Table 2.a

ASSUMED FRACTIONAL TRUNCATION ERROR IN YY ELEMENTS= 1E-08

3 BY 3 YY MATRIX IS SINGULAR.

RADIANCE ESTIMATES ARE DERIVED FROM LW CHANNEL AND TOTAL CHANNEL.

THE FIELD PROBABILITY MATRIX FILE NAME IS "OCM.Z45.PROB24"

THE SCANNER RESPONSE MATRIX FILE NAME IS "MID-LAT.OCEAN.36FIELDS"

THERE ARE 25 MEASUREMENT TRIPLETS.

ACTUAL SW	EST SW	SW ERROR	ACTUAL LW	EST LW	LW ERROR
0	0	0	54.147	54.150	-2.716E-03
0	0	0	77.040	77.029	.010
0	0	0	80.417	80.385	.032
0	0	0	80.417	80.385	.032
0	0	0	97.985	98.022	-.037
0	0	0	71.543	71.539	4.287E-03
0	0	0	54.147	54.150	-2.716E-03
0	0	0	87.532	87.530	1.544E-03
0	0	0	60.532	60.538	-5.268E-03
0	0	0	60.437	60.442	-5.050E-03
0	0	0	97.985	98.022	-.037
0	0	0	85.020	85.015	5.385E-03
0	0	0	77.040	77.029	.010
0	0	0	80.417	80.385	.032
0	0	0	97.985	98.022	-.037
0	0	0	60.532	60.538	-5.268E-03
0	0	0	80.417	80.385	.032
0	0	0	97.985	98.022	-.037
0	0	0	60.437	60.442	-5.050E-03
0	0	0	80.417	80.385	.032
0	0	0	80.417	80.385	.032
0	0	0	87.532	87.530	1.544E-03
0	0	0	77.040	77.029	.010
0	0	0	71.543	71.539	4.287E-03
0	0	0	60.437	60.442	-5.050E-03

Table 2.b

(PERCENTAGES ARE OF MEAN SW OR LW RADIANCES.)

THE LW RADIANCES ARE BIASED BY -2.629E-03 OR -3.425E-03 %

THE LW STANDARD DEVIATION IS .022 OR .029 %

THE LW STANDARD DEVIATION EXCLUDING BIAS IS .022

MATRIX OF CHANNEL INFLUENCES ON ESTIMATES

	TOTAL CHANNEL	SW CHANNEL	LW CHANNEL
SW EST	0	0	0
LW EST	1.22436789	0	-.174493093

SW POPULATION BIAS= 0
LW POPULATION BIAS= -5.02077E-04 OR -6.69776E-04 %

SW POPULATION STD DEV= 0
LW POPULATION STD DEV= .01719 OR .02294 %

Table 3.a

ASSUMED FRACTIONAL TRUNCATION ERROR IN YY ELEMENTS= 1E-08

THE FIELD PROBABILITY MATRIX FILE NAME IS "OCHM.Z45.PROB27"

THE SCANNER RESPONSE MATRIX FILE NAME IS "MID-LAT.OCEAN.36FIELDS"

THERE ARE 25 MEASUREMENT TRIPLETS.

ACTUAL SW	EST SW	SW ERROR	ACTUAL LW	EST LW	LW ERROR
29.562	29.492	.070	87.532	87.535	-3.829E-03
29.330	29.360	-.029	97.985	98.021	-.036
29.330	29.322	8.158E-03	80.417	80.389	.028
29.562	29.492	.070	78.784	78.779	5.619E-03
37.171	37.117	.054	77.040	77.040	-2.762E-04
37.171	37.108	.063	54.147	54.163	-.015
29.777	29.814	-.036	97.985	98.022	-.037
37.691	37.768	-.077	87.532	87.536	-4.525E-03
29.777	29.800	-.022	78.784	78.774	.010
37.691	37.767	-.075	77.040	77.035	5.330E-03
37.275	37.262	.012	60.437	60.449	-.011
37.691	37.744	-.052	80.417	80.395	.022
29.641	29.667	-.026	54.147	54.151	-3.738E-03
29.633	29.671	-.037	78.784	78.773	.010
29.562	29.492	.070	87.532	87.535	-3.829E-03
29.641	29.684	-.042	85.020	85.013	7.351E-03
29.562	29.506	.056	97.985	98.026	-.041
29.777	29.800	-.023	87.532	87.531	6.019E-04
37.275	37.262	.012	60.437	60.449	-.011
29.330	29.350	-.019	65.705	65.702	3.138E-03
29.562	29.495	.066	65.705	65.707	-2.281E-03
37.691	37.768	-.076	78.784	78.779	4.923E-03
29.777	29.807	-.029	85.020	85.014	6.236E-03
29.330	29.322	8.158E-03	80.417	80.389	.028
29.330	29.346	-.016	87.532	87.530	1.590E-03

Table 3.b

THE SW RADIANCES ARE BIASED BY 2.937E-03 OR 9.156E-03%

(PERCENTAGES ARE OF MEAN SW OR LW RADIANCES.)

THE LW RADIANCES ARE BIASED BY 1.490E-03 OR 1.888E-03 %

THE SW STANDARD DEVIATION IS .048 OR .151 %

THE LW STANDARD DEVIATION IS .017 OR .022 %

THE SW STANDARD DEVIATION EXCLUDING BIAS IS .048

THE LW STANDARD DEVIATION EXCLUDING BIAS IS .017

MATRIX OF CHANNEL INFLUENCES ON ESTIMATES

	TOTAL CHANNEL	SW CHANNEL	LW CHANNEL
SW EST	.0224043801	1.63077869	-.0300852433
LW EST	1.22373034	-1.40781623	-.173524708

SW POPULATION BIAS= 7.61532E-04 OR 2.365E-03 %

LW POPULATION BIAS= 2.04801E-03 OR 2.750E-03 %

SW POPULATION STD DEV= .04731 OR .146 %

LW POPULATION STD DEV= .01564 OR .021 %

Table 4.a

ASSUMED FRACTIONAL TRUNCATION ERROR IN YY ELEMENTS= 1E-08

3 BY 3 YY MATRIX IS SINGULAR.

RADIANCE ESTIMATES ARE DERIVED FROM LW CHANNEL AND TOTAL CHANNEL.

THE FIELD PROBABILITY MATRIX FILE NAME IS "OCHM.Z45.PROB27"

THE SCANNER RESPONSE MATRIX FILE NAME IS "MID-LAT.OCEAN.36FIELDS"

THERE ARE 25 MEASUREMENT TRIPLETS.

ACTUAL SW	EST SW	SW ERROR	ACTUAL LW	EST LW	LW ERROR
0	0	0	65.705	65.704	7.131E-04
0	0	0	65.705	65.704	7.131E-04
0	0	0	71.543	71.540	2.979E-03
0	0	0	60.532	60.539	-6.413E-03
0	0	0	87.532	87.532	7.748E-07
0	0	0	54.147	54.151	-3.754E-03
0	0	0	54.147	54.151	-3.754E-03
0	0	0	85.020	85.016	3.873E-03
0	0	0	78.784	78.774	.010
0	0	0	78.784	78.774	.010
0	0	0	54.147	54.151	-3.754E-03
0	0	0	65.705	65.704	7.131E-04
0	0	0	80.417	80.386	.031
0	0	0	97.985	98.024	-.038
0	0	0	71.543	71.540	2.979E-03
0	0	0	97.985	98.024	-.038
0	0	0	54.147	54.151	-3.754E-03
0	0	0	71.543	71.540	2.979E-03
0	0	0	60.437	60.443	-6.193E-03
0	0	0	60.532	60.539	-6.413E-03
0	0	0	87.532	87.532	7.748E-07
0	0	0	65.705	65.704	7.131E-04
0	0	0	77.040	77.031	9.376E-03
0	0	0	71.543	71.540	2.979E-03
0	0	0	85.020	85.016	3.873E-03

Table 4.b

(PERCENTAGES ARE OF MEAN SW OR LW RADIANCES.)

THE LW RADIANCES ARE BIASED BY 1.095E-03 OR 1.519E-03 %

THE LW STANDARD DEVIATION IS .013 OR .018 %

THE LW STANDARD DEVIATION EXCLUDING BIAS IS .013

MATRIX OF CHANNEL INFLUENCES ON ESTIMATES

	TOTAL CHANNEL	SW CHANNEL	LW CHANNEL
SW EST	0	0	0
LW EST	1.22441104	0	-.174529083

SW POPULATION BIAS= 0
LW POPULATION BIAS= -3.23628E-04 OR -4.34586E-04 %

SW POPULATION STD DEV= 0
LW POPULATION STD DEV= .01593 OR .02139 %

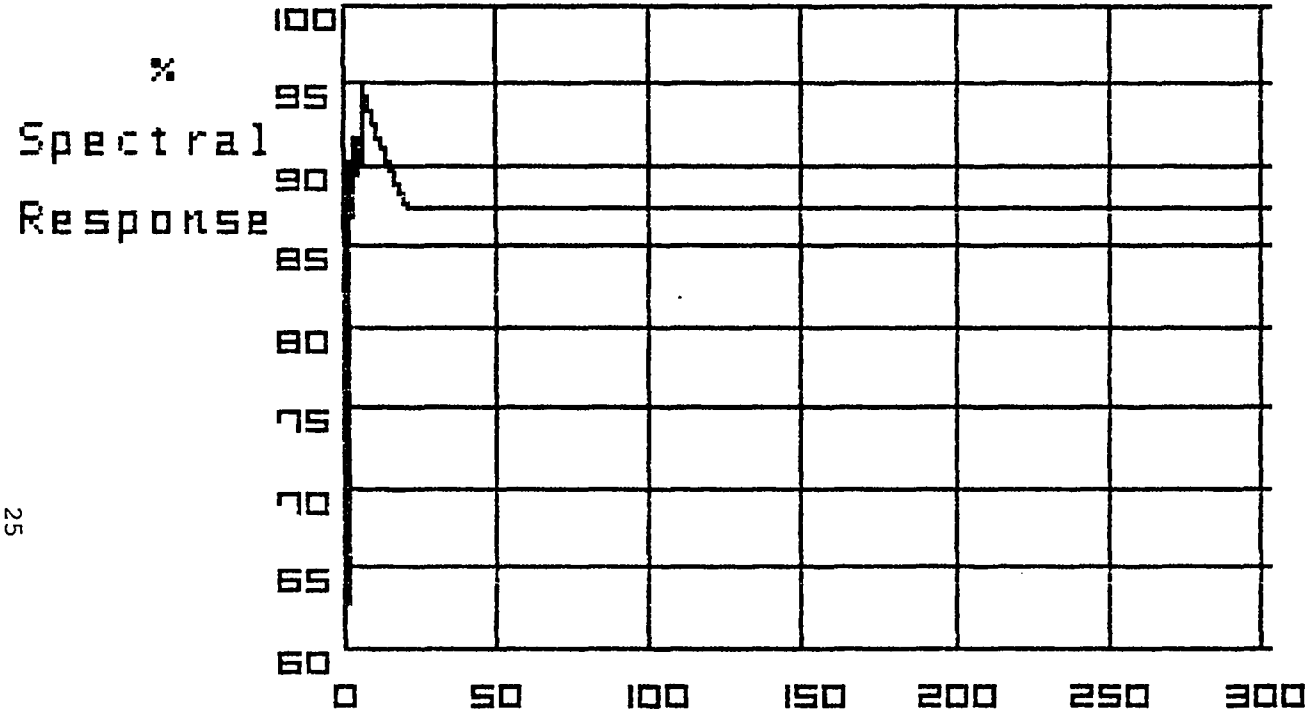

Fig. 1.a- TOTAL CHANNEL RESPONSE
FROM 0.15 TO 300 MICRONS

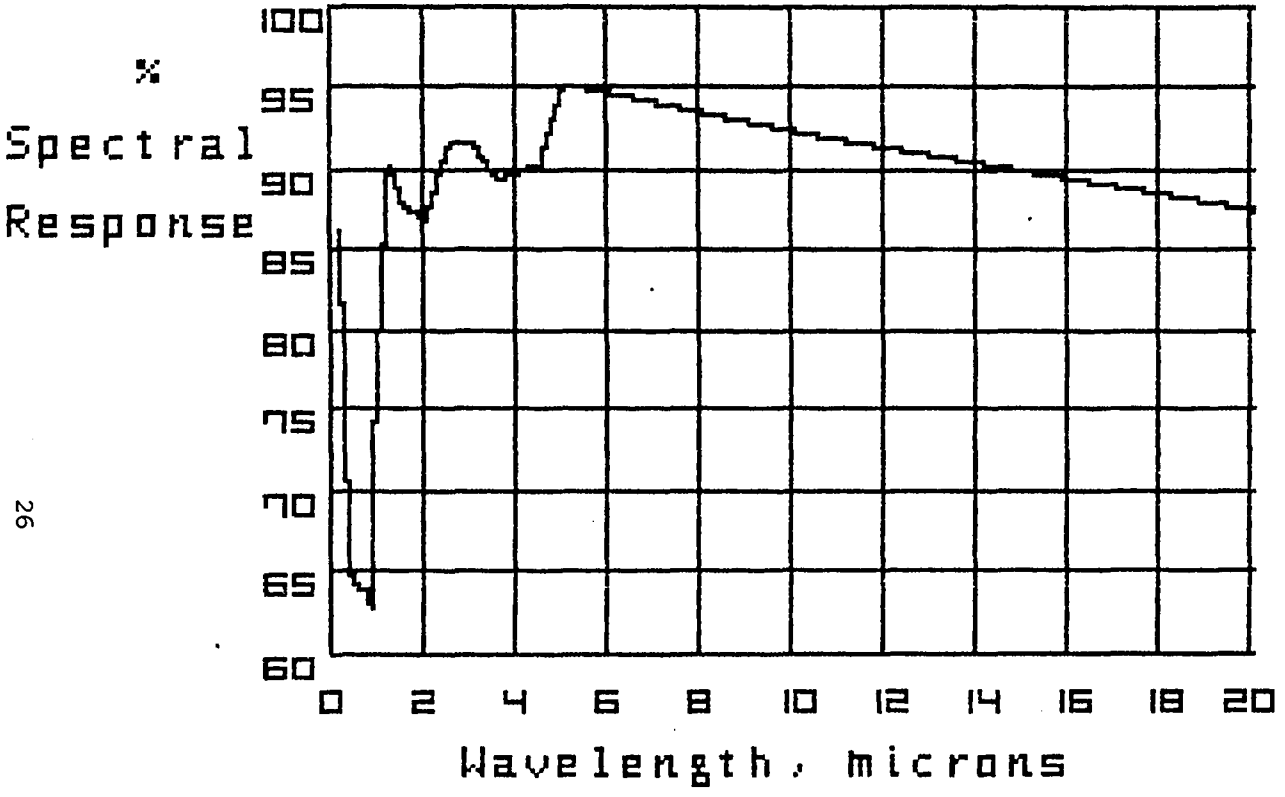

Fig. 1.b- TOTAL CHANNEL RESPONSE
FROM 0.15 TO 20 MICRONS

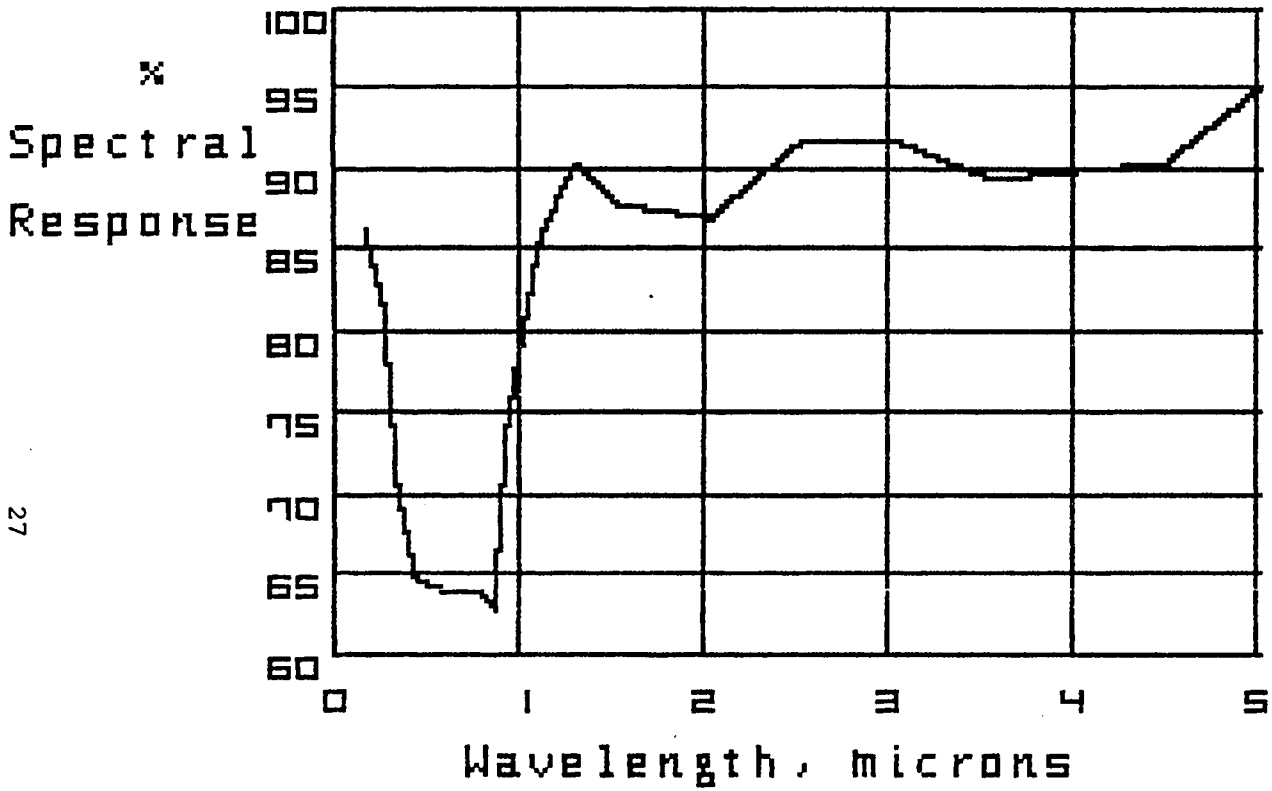

Fig. 1.c- TOTAL CHANNEL RESPONSE
FROM ø.1s TO s MICRONS

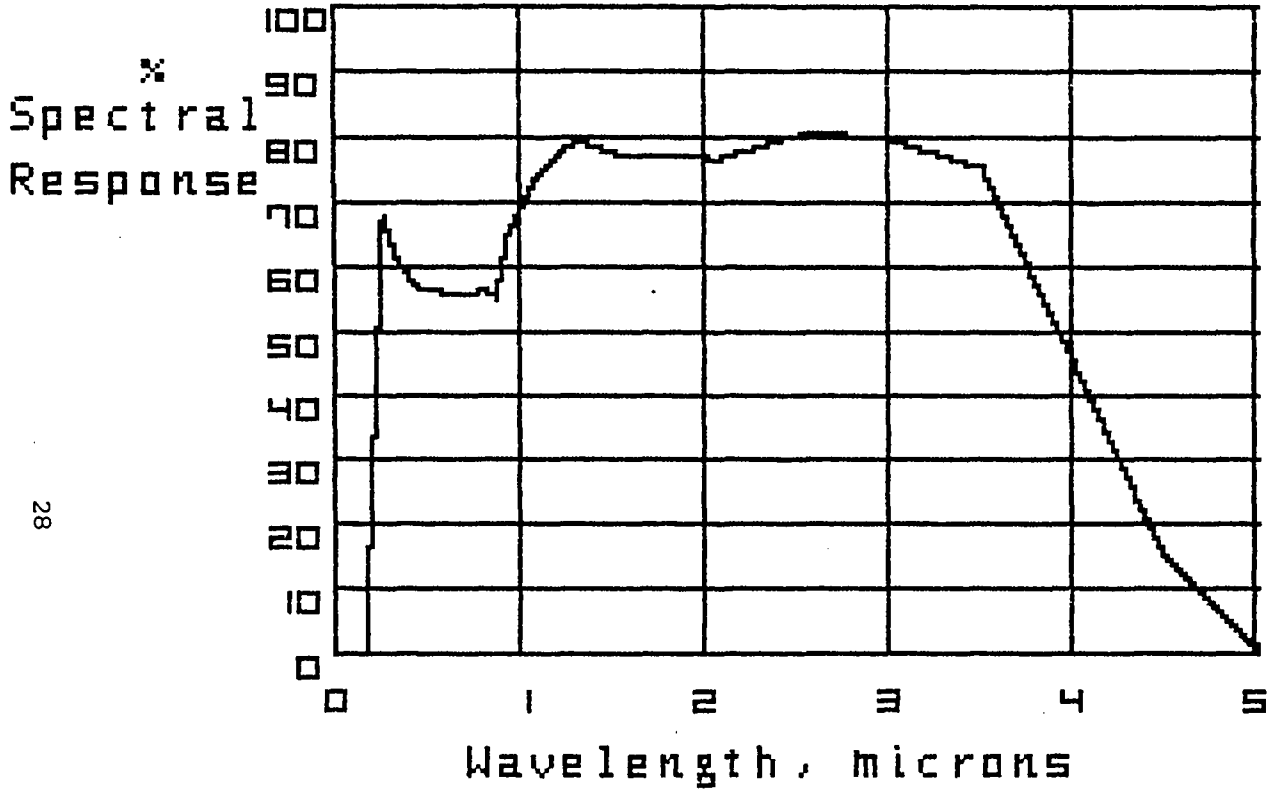

Fig. 1.d- SHORTWAVE CHANNEL RESPONSE FROM ø.1s TO s MICRONS

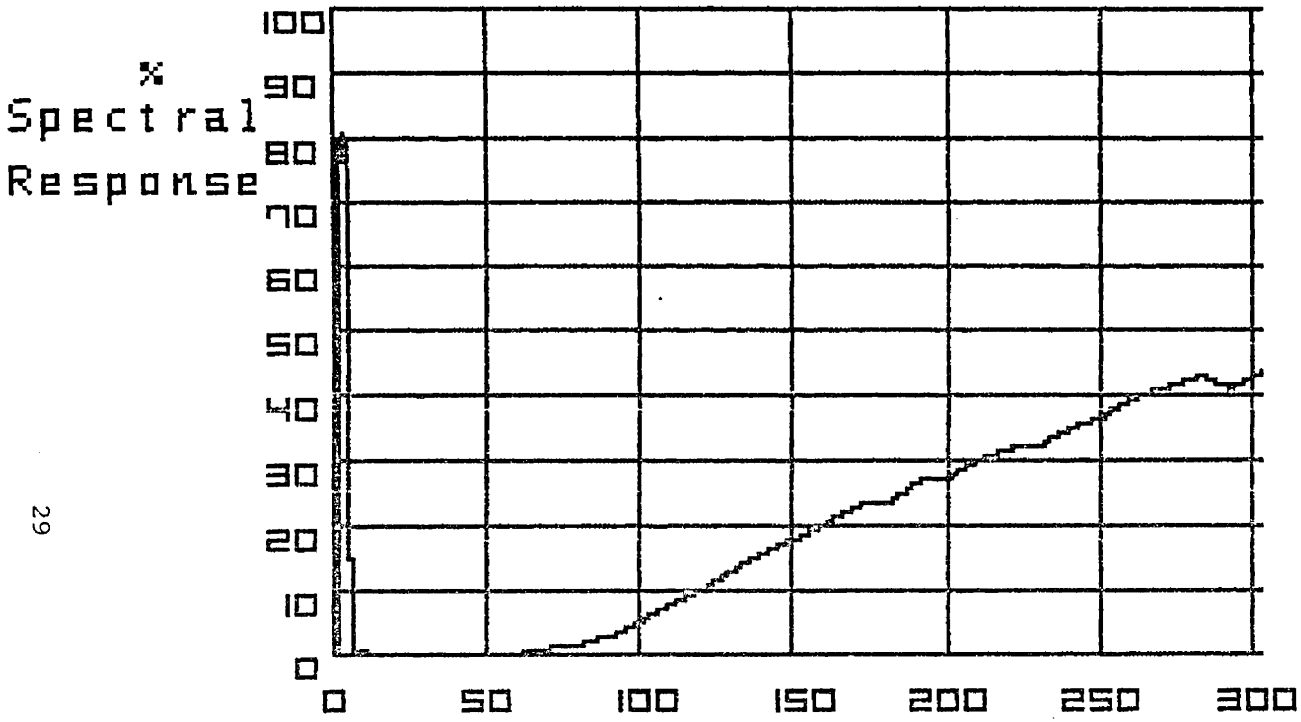

Fig. 1.e- SHORTWAVE CHANNEL RESPONSE FROM 0.15 TO 300 MICRONS

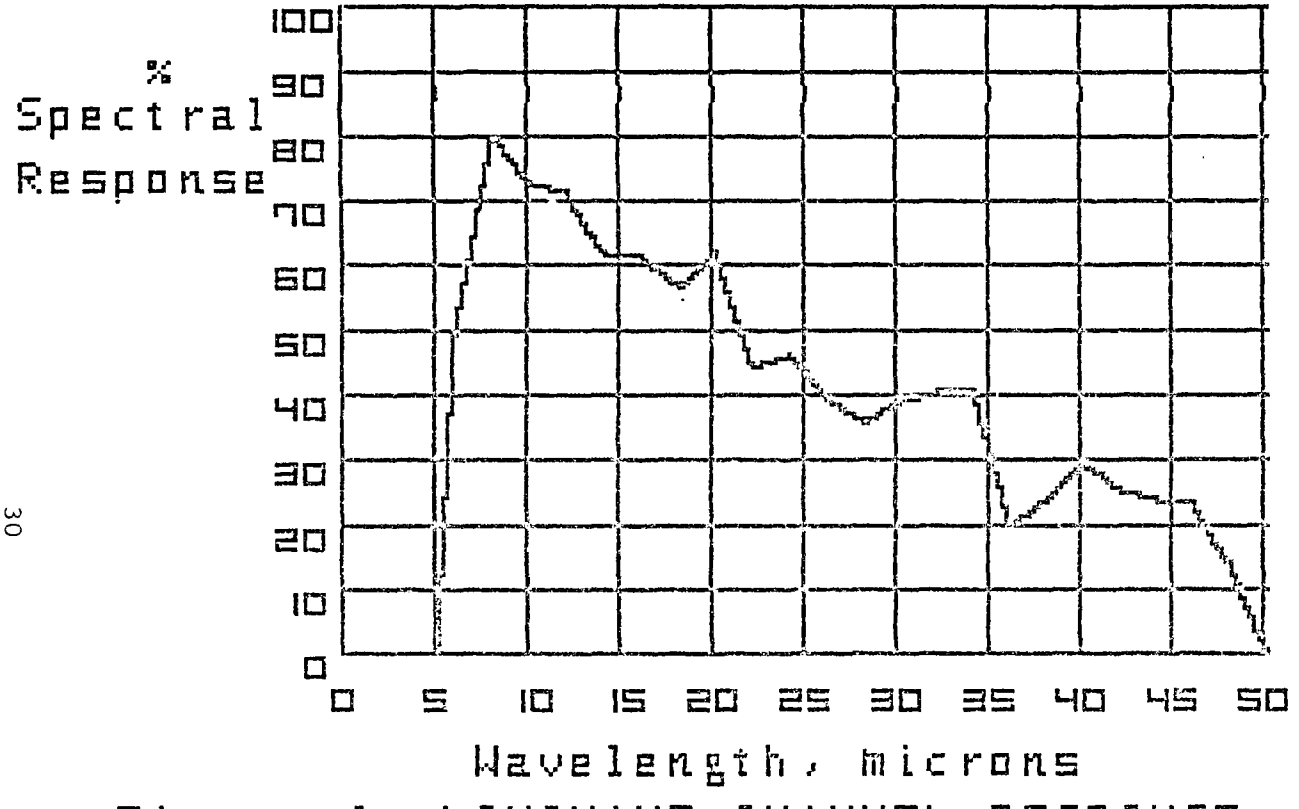

Fig. 1.f- LONGWAVE CHANNEL RESPONSE FROM 0.15 TO 50 MICRONS

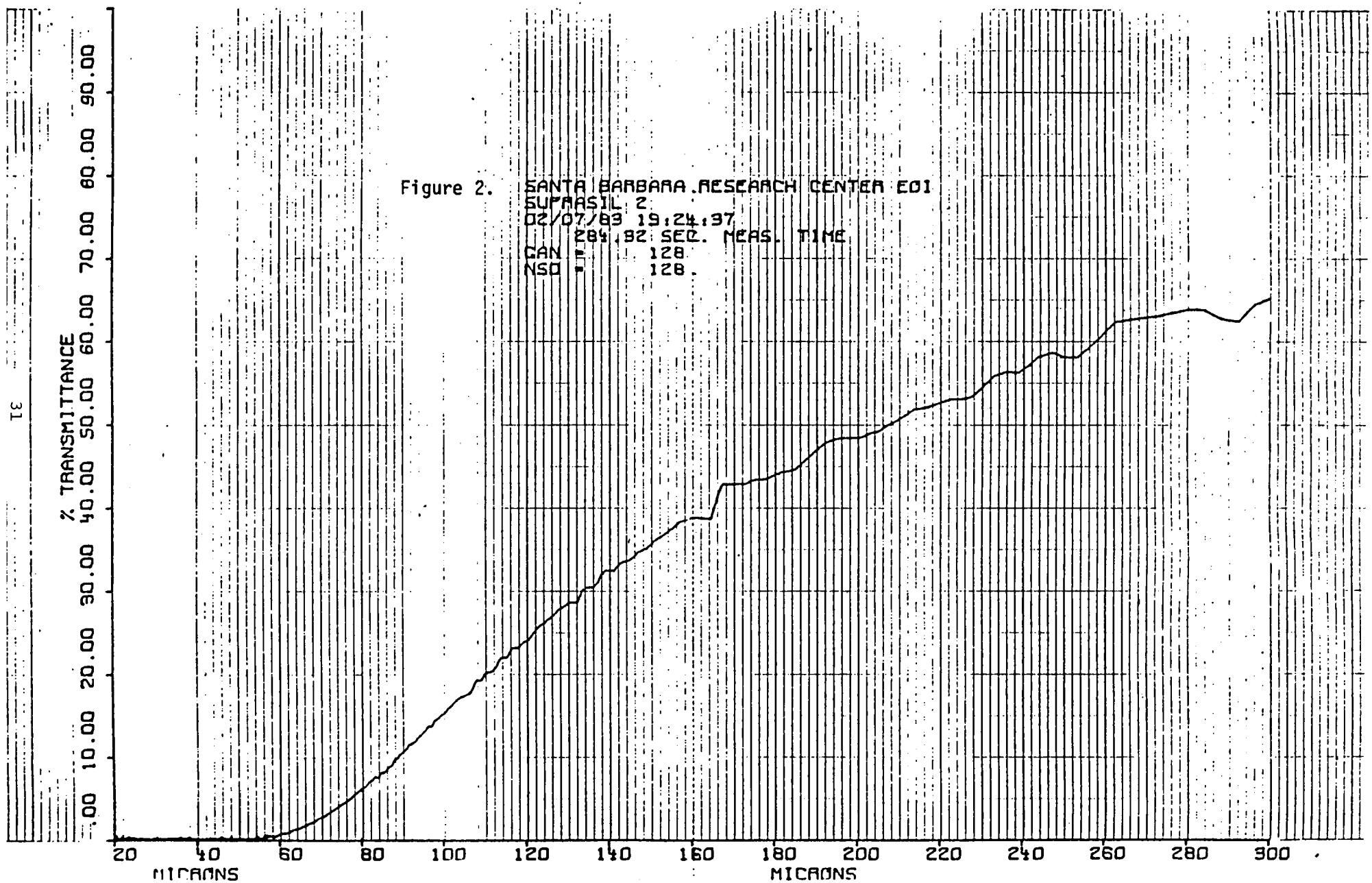
SANTA BARBARA RESEARCH CENTER EOI
SUPRASIL 2
02/07/83 19:24:37
284.82 SEC. MEAS. TIME
CAN = 128
NSO = 128.
% TRANSMITTANCE
00 10.00 20.00 30.00 40.00 50.00 60.00 70.00 80.00 90.00
20 40 60 80 100 120 140 160 180 200 220 240 260 280 300
MICRONS
MICRONS

Figure 2.

1. Report No.	2. Government Accession No.	3. Recipient's Catalog No.
NASA TM-85781		

4. Title and Subtitle	5. Report Date
A Robust Pseudo-Inverse Spectral Filter Applied To The Earth Radiation Budget Experiment (ERBE) Scanning Channels	March 1984
	6. Performing Organization Code 619-12-30-03
7. Author(s) Lee M. Avis, Richard N. Green, John T. Suttles, and Shashi K. Gupta	8. Performing Organization Report No.
9. Performing Organization Name and Address NASA Langley Research Center Hampton, VA 23665	10. Work Unit No.
	11. Contract or Grant No.
12. Sponsoring Agency Name and Address National Aeronautics and Space Administration Washington, DC 20546	13. Type of Report and Period Covered Technical Memorandum
	14. Sponsoring Agency Code

15. Supplementary Notes

Lee M. Avis, Richard N. Green, and John T. Suttles, NASA Langley Research Center
Shashi K. Gupta, Kentron International, Inc., Kentron Technical Center, Hampton, Virginia

16. Abstract

Computer simulations of a least squares estimator operating on the ERBE scanning channels are discussed. The estimator is designed to minimize the errors produced by non-ideal spectral response to spectrally varying and uncertain radiant input. The three ERBE scanning channels cover, respectively, a shortwave band from 0.18 to 5 microns, a longwave band from 5 to 50 microns, and a "total" band from 0.15 to beyond 1000 microns, from which the pseudo-inverse spectral filter estimates the radiance components in the shortwave band and a longwave band (5 to 1000 microns).

The radiance estimator draws on instantaneous field of view (IFOV) scene-type information supplied by another algorithm of the ERBE software, and on a priori probabilistic models of the responses of the scanning channels to the IFOV scene types for given Sun-scene spacecraft geometry.

The pseudo-inverse spectral filter has been found to be stable, tolerant of errors in scene identification and in channel response modeling, and, in the absence of such errors, to yield minimum variance and essentially unbiased radiance estimates.

17. Key Words (Suggested by Author(s))	18. Distribution Statement
Earth Radiation Budget Satellite Sensors Spectral Correction	Unclassified - Unlimited Subject Category 47

19. Security Classif. (of this report)	20. Security Classif. (of this page)	21. No. of Pages	22. Price
Unclassified	Unclassified	32	A03

For sale by the National Technical Information Service, Springfield, Virginia 22161